Journal of Applied Polymer Science

Relationship Between Branch Length and the Compatibilizing Effect of Polypropylene-*g*-Polystyrene Graft Copolymer on Polypropylene/Polystyrene Blends

Lu Wang,[1,2] Haiying Tan,[1,2] Jiang Gong,[1,2] Tao Tang[1]

[1]State Key Laboratory of Polymer Physics and Chemistry, Changchun Institute of Applied Chemistry, Chinese Academy of Sciences, Changchun 130022, China

[2]University of Chinese Academy of Sciences, Beijing 100049, China

Correspondence to: T. Tang (E-mail: ttang@ciac.ac.cn)

ABSTRACT: Three polypropylene-*g*-polystyrene (PP-*g*-PS) graft copolymers with the same branch density but different branch lengths were evaluated as compatibilizing agents for PP/PS blends. The morphological and rheological results revealed that the addition of PP-*g*-PS graft copolymers significantly reduced the PS particle size and enhanced the interfacial adhesion between PP and PS phases. Furthermore, it is verified that the branch length of PP-*g*-PS graft copolymer had opposite effects on its compatibilizing effect: on one hand, increasing the branch length could improve the compatibilizing effect of graft copolymer on PP/PS blends, demonstrated by the reduction of PS particle size and the enhancement of interfacial adhesion; on the other hand, increasing the branch length would increase the melt viscosity of PP-*g*-PS graft copolymer, which prevented it from migrating effectively to the interface of blend components. Additionally, the crystallization and melting behaviors of PP and PP/PS blends were compared. © 2013 Wiley Periodicals, Inc. J. Appl. Polym. Sci. **2014**, *131*, 40126.

KEYWORDS: blends; compatibilization; rheology; polyolefins; polystyrene

Received 23 July 2013; accepted 26 October 2013

DOI: 10.1002/app.40126

INTRODUCTION

In the past decades, polymer blending has been attracting a lot of attention because it offers a convenient alternative to developing new high-performance materials. Isotactic polypropylene (iPP) is one of the most widespread commercial polymers due to its outstanding physical and chemical properties such as high melting point, low density, high tensile modulus, excellent chemical resistance, and low cost. However, its toughness, strength, and stiffness are not sufficient for applications as an engineering plastic. PS, a rigid polymer produced in large amount with low cost, can be used to reinforce PP.[1] However, PP and polystyrene (PS) are immiscible, and their blends usually have poor mechanical properties due to serious phase separation and low interfacial adhesion. The properties of immiscible blends would be improved after adding compatibilizing agents. Usually, such compatibilizers have blocks or graft segments that are chemically identical to those in the respective phases and work by improving the interfacial adhesion.[2] Poly (styrene-*b*-butadiene-*b*-styrene) (SBS),[3–7] poly(styrene-*b*-ethylene-*co*-butylene-*b*-styrene) (SEBS),[3,7–9] poly(styrene-*b*-ethylene-*co*-propylene) (SEP),[7,10,11] poly(styrene-*b*-isoprene-*b*-styrene) (SIS),[6] and PP-*g*-PS copolymers[1,2,12–21] can be used as compatibilizing agents for PP/PS blends. Among which, PP-*g*-PS graft copolymer, composed of a PP backbone and PS branches, is an ideal compatibilizer for PP/PS blends due to the good compatibilities of PP backbone and PS branches with PP bulk and PS bulk, respectively.

Although extensive studies have been reported in the literature about the compatibilizing effect of PP-*g*-PS graft copolymer on PP/PS blends, the systematic study about the relationship between molecular structure and the compatibilizing effect of PP-*g*-PS graft copolymer has been seriously limited. This is ascribed to the difficulty of preparing PP-*g*-PS graft copolymers with well-defined molecular structures. Schulze and coworkers reported the metallocene catalyzed copolymerization of propylene with allyl-terminated polystyrene macromonomer to synthesize PP-*g*-PS graft copolymers with well-defined molecular structures.[12,22] Chung and coworkers developed another route for preparing PP-*g*-PS graft copolymers with well-defined molecular structures. A poly(propylene-*co*-*p*-methylstyrene) copolymer was first synthesized using heterogeneous Ziegler–Natta catalyst and subsequently lithiated in the *p*-methyl groups of *p*-methylstyrene (*p*-MS) units for initiating anionic polymerization of styrene.[23] Kaneko et al. first copolymerized propylene with 10-undecen-1-ol to synthesize the PP-OH copolymer, and

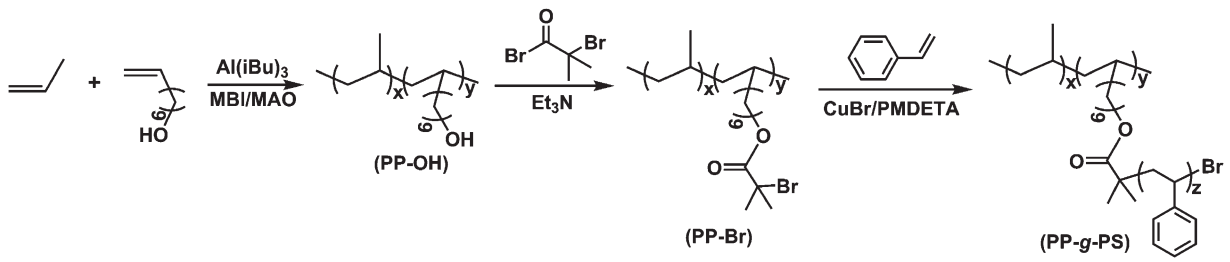

Scheme 1. Synthesis route for PP-*g*-PS graft copolymers.

the hydroxyl groups in the resulting PP-OH copolymer were converted into the 2-bromoisobutyrate groups. The PP-*g*-PS graft copolymers were then prepared by atom transfer radical polymerization (ATRP).[24]

Recently, we synthesized several polypropylene-*g*-polystyrene (PP-*g*-PS) graft copolymers with well-defined molecular structures, based on the same PP-Br macroinitiator, via a combination of metallocene catalyzed polymerization and ATRP.[25] In this work, the obtained PP-*g*-PS graft copolymers with the same branch density but different branch lengths were employed to compatibilize PP/PS blends. The relationship between branch length and the compatibilizing effect of PP-*g*-PS graft copolymer on PP/PS blends were systematically investigated.

EXPERIMENTAL

Materials

iPP ($M_w = 3.07 \times 10^5$ g/mol, polydispersity index = 3.13) powder was supplied by Daqing Petrochemical Corp., China. Atactic polystyrene pellets (PS, $M_w = 3.72 \times 10^5$ g/mol, polydispersity index = 1.78) were purchased from Zhenjiang Qimei Chemical Co., Ltd., China. PP-*g*-PS samples were synthesized according to the method shown in Scheme 1. In the first step, poly(propylene-*co*-10-undecen-1-ol) copolymer (PP-OH) was obtained through the copolymerization of propylene with aluminum-capped 10-undecen-1-ol using the catalyst system of *rac*-Me_2Si(2-MeBenz[*e*]Ind)$_2ZrCl_2$ (MBI)/MAO. In the second step, the hydroxyl group in the resulting PP-OH copolymer was converted into the 2-bromoisobutyrate group by reacting with an excess amount of 2-bromoisobutyryl bromide in the presence of triethylamine. Three PP-*g*-PS graft copolymers were then synthesized based on the same PP-Br macroinitiator via ATRP. The details are shown in another paper.[25] The nomenclature denotes the topology of the graft polymer which is described as PP-*xg*-PS*y*: The symbol *x* denotes the branch density (defined as the average number of branches per 10,000 carbons in the PP backbone), and *y* denotes the branch length (defined as the average molecular weight of branches, kg/mol). The characteristics of PP-*g*-PS samples are shown in Table I.

Polymer Blending

The PP, PS, and PP-*g*-PS polymers were dissolved in toluene at 110°C under an argon atmosphere for an hour, and then poured into excess ethanol to precipitate the polymer blends. The polymer blends were filtered, washed with ethanol for several times, and then dried under vacuum at 60°C for 24 h. Besides, neat PP sample was also treated by the same process. The nomenclature denotes the composition of the blend which is described as PP/PS/PP-*xg*-PS*y*-*z*: The symbol *z* denotes the concentration of PP-*xg*-PS*y* graft copolymer in the blend. The weight ratio of PP and PS in all the blends was fixed at 70/30.

Chracterization

Melting temperatures (T_m) and crystallization temperatures (T_c) of the samples were determined by differential scanning calorimetry (DSC) using a Mettler DSC 1 instrument operating at a heating rate of 10 °C/min from 25 to 200°C under a nitrogen atmosphere.

Rheological measurements were preformed on an ARES-G2 rheometer (TA Instruments) at 180°C. The parallel plate with a diameter of 25 mm and a gap height of 0.8 mm was used. The

Table I. Summary of Characterization Results by DSC, SEC, and Rheology Measurements for PP-Br and PP-*g*-PS Copolymers

Sample	St content[a] (wt %)	T_m[b] (°C)	$\Delta H_{m,\text{whole}}$[b] (J g^{-1})	$\Delta H_{m,\text{PP}}$[c] (J g^{-1})	M_w[d] (10^4 g mol^{-1})	M_w/M_n[d]	$\eta^*_{0.05\ \text{rad/s}}$[e] ($10^4$ Pa s)	$G'_{0.05\ \text{rad/s}}$[f] (Pa)
PP-Br	0	147.7	87.7	87.7	31.9	1.96	1.19	59
PP-7*g*-PS2.5	7.8	147.1	81.8	88.7	33.1	2.00	4.97	722
PP-7*g*-PS4.4	12.8	147.1	77.2	88.5	34.4	2.02	64.58	25,930
PP-7*g*-PS6.0	16.7	146.5	73.1	87.8	35.0	2.05	74.67	33,117

[a] Weight fraction of St in the resulting graft copolymer.
[b] Determined by DSC measurements.
[c] $\Delta H_{m,\text{PP}} = \Delta H_{m,\text{whole}}$/wt % of PP in the obtained graft copolymer.
[d] Measured by SEC with a differential refractive index detector.
[e] The η^* value at the frequency of 0.05 rad/s obtained by rheology measurements.
[f] The G′ value at the frequency of 0.05 rad/s obtained by rheology measurements.

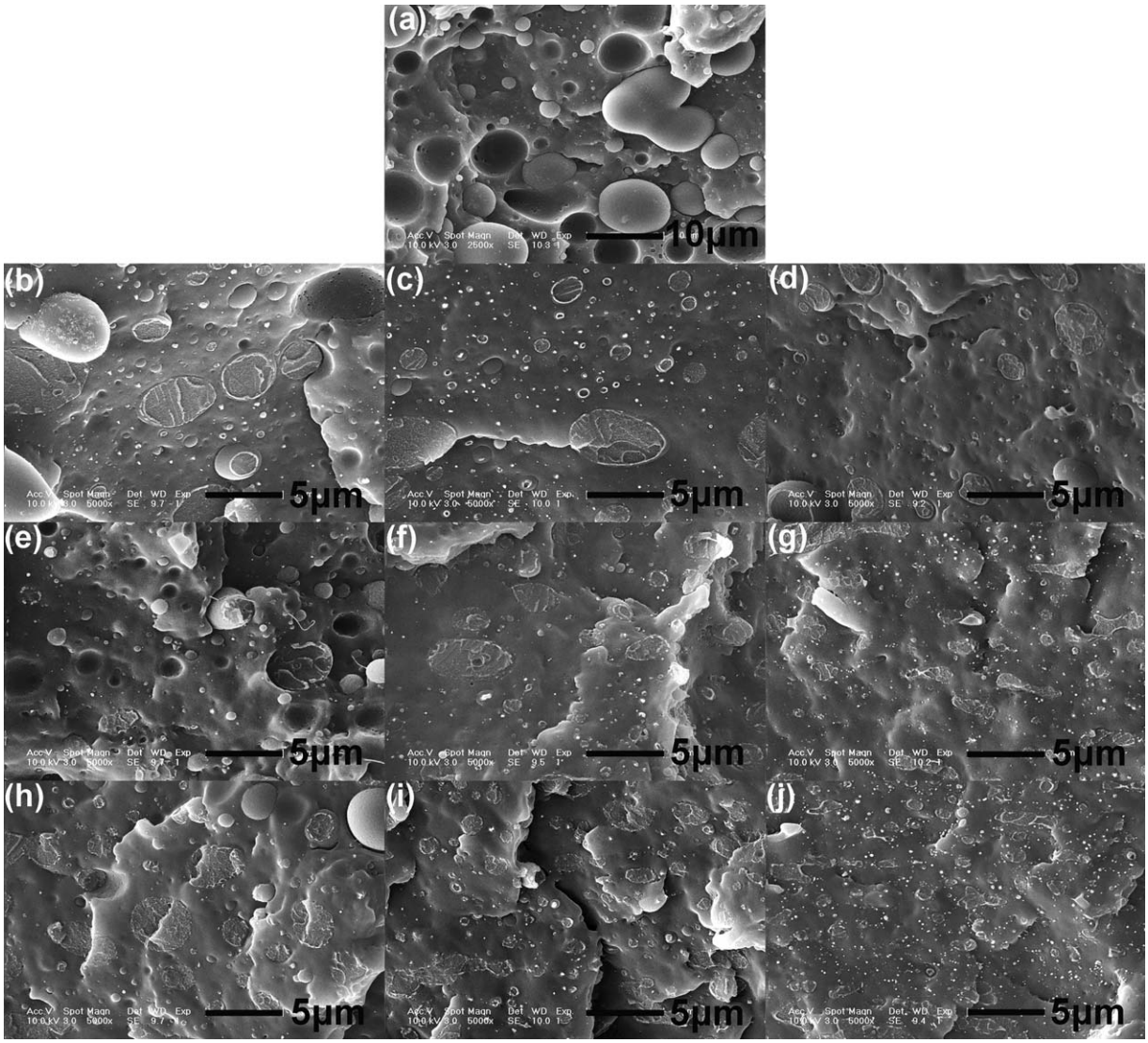

Figure 1. Morphology of the PP/PS (70/30) blends uncompatibilized and compatibilized with the PP-*g*-PS graft copolymers: (a) PP/PS (70/30), (b) PP/PS/PP-7*g*-PS2.5-1, (c) PP/PS/PP-7*g*-PS2.5-2.5, (d) PP/PS/PP-7*g*-PS2.5-5, (e) PP/PS/PP-7*g*-PS4.4-1, (f) PP/PS/PP-7*g*-PS4.4-2.5, (g) PP/PS/PP-7*g*-PS4.4-5, (h) PP/PS/PP-7*g*-PS6.0-1, (i) PP/PS/PP-7*g*-PS6.0-2.5, and (j) PP/PS/PP-7*g*-PS6.0-5 blends.

test samples were first treated with 0.2 wt % Irganox B215 antioxidant and formed into disks with a diameter of 25 mm and a thickness of 1 mm by compression-molding at 180°C and 10 MPa. Then, the samples were cooled quickly to room temperature while still under 10 MPa. The range of the frequency sweeps was from 0.05 to 100 rad/s. A strain of 1% was used, which was in the linear viscoelastic regime for all samples. The rheometer oven was purged with dry nitrogen to avoid degradation of samples during measurements.

The morphology of polymer blends was characterized by a XL 30 ESEM FEG scanning electron microscope (SEM). The compression-molded blend samples were fractured in liquid nitrogen. The fractured surfaces were coated with a thin layer of gold before SEM observation. Particle size analysis was performed with ImageJ software. The number-average diameter (d_n) of PS particles in the blend can be calculated by the following equation:

$$d_n = \frac{\sum_i n_i d_i}{\sum_i n_i} \quad (1)$$

where d_i is the diameter of each PS particle, and n_i is the number of particles with a diameter of d_i.

RESULTS AND DISCUSSION

Morphology of PP/PS Blends

Aiming at investigating the relationship between branch length and the compatibilizing effect of PP-*g*-PS graft copolymer on PP/PS blends, three PP-*g*-PS graft copolymers possessing identical branch density but different branch lengths were used to compatibilize PP/PS blends. The SEM images of cryogenically fractured surfaces of PP/PS (70/30) blends, uncompatibilized and compatibilized with the PP-*g*-PS graft copolymers, are presented in Figure 1. The PS particle size distributions for all the blends are illustrated in Figure 2, and the calculated number-average particle diameters (d_n) are summarized in Table II. The

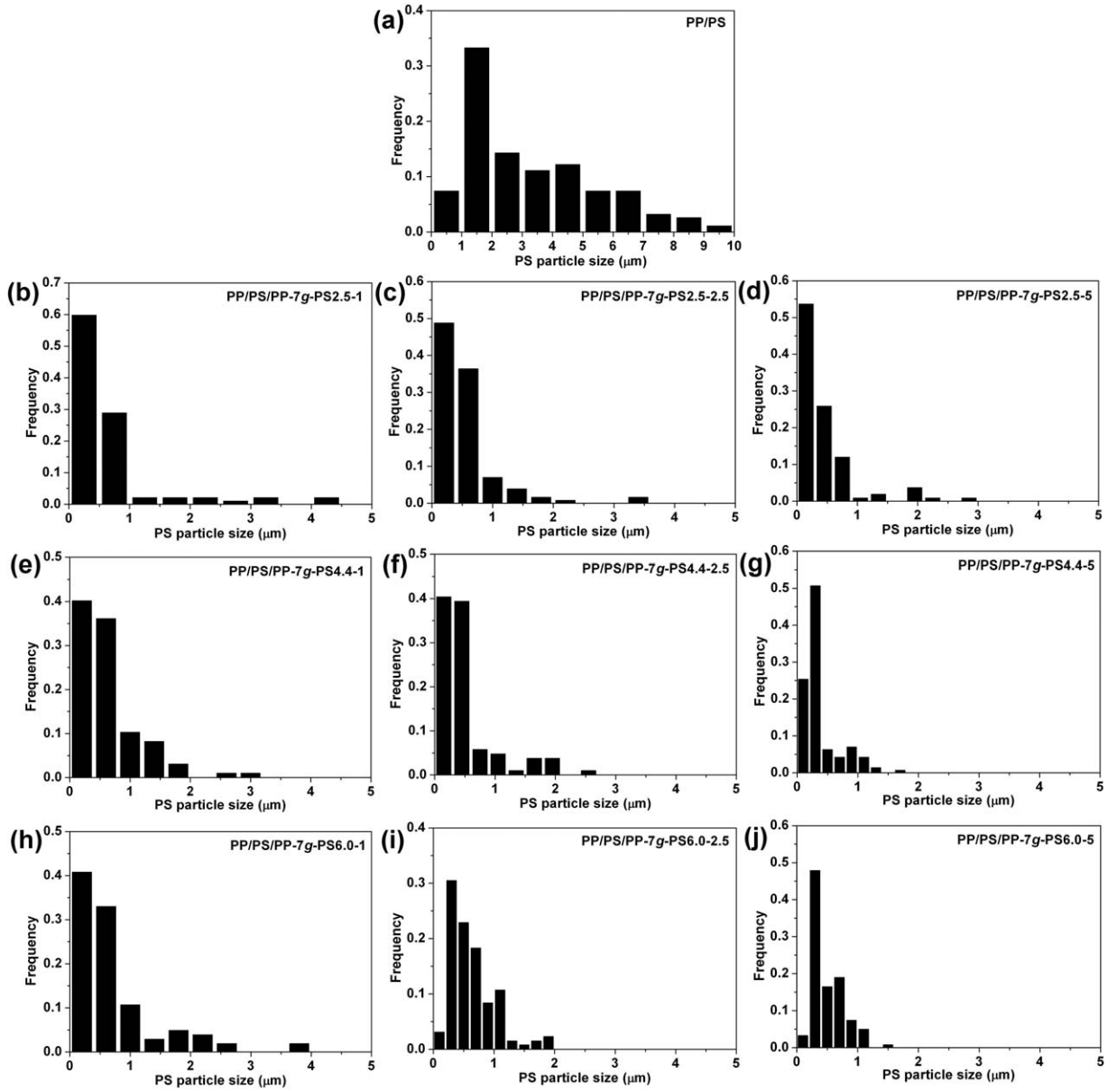

Figure 2. PS particle size distributions of PP/PS (70/30) blends uncompatibilized and compatibilized with the PP-*g*-PS graft copolymers: (a) PP/PS (70/30), (b) PP/PS/PP-7*g*-PS2.5-1, (c) PP/PS/PP-7*g*-PS2.5-2.5, (d) PP/PS/PP-7*g*-PS2.5-5, (e) PP/PS/PP-7*g*-PS4.4-1, (f) PP/PS/PP-7*g*-PS4.4-2.5, (g) PP/PS/PP-7*g*-PS4.4-5, (h) PP/PS/PP-7*g*-PS6.0-1, (i) PP/PS/PP-7*g*-PS6.0-2.5, and (j) PP/PS/PP-7*g*-PS6.0-5 blends.

uncompatibilized PP/PS (70/30) blend showed the typical characteristics of an immiscible blend [Figure 1(a)].[1,2,21,26–31] The size of the PS particle was large ($d_n = 3.28$ μm) and had a broad distribution [Figure 2(a)]. The interface between the PP matrix and the PS particle was smooth and clear, and the holes formed during fracture indicated low adhesion between the two phases and poor stress transfer across the interface.

Upon addition of PP-*g*-PS graft copolymers to the PP/PS (70/30) blend, the PS particle sizes were significantly decreased, and the particle size distributions were obviously narrowed [Figures 1(b–j) and 2(b–j)]. In addition, most PS particles were fractured, indicating that the interfacial adhesion was prominently enhanced. From Figures 1(b–d) and 2(b–d), it can be found that increasing the concentration of PP-7*g*-PS2.5 graft copolymer reduced the PS particle size and narrowed the particle size distribution. Similar results can be obtained by comparing the morphology of PP/PS (70/30) blends compatibilized with different concentrations of PP-7*g*-PS4.4 [Figures 1(e–g) and 2(e–g)] or PP-7*g*-PS6.0 [Figures 1(h–j) and 2(h–j)] graft copolymers.

Comparing the morphology of PP/PS (70/30) blends compatibilized with 1 wt % PP-*g*-PS graft copolymer, one can note that the PP-7*g*-PS4.4 graft copolymer was more effective in reducing the PS particle size than both PP-7*g*-PS2.5 and PP-7*g*-PS6.0

Table II. Summary of Characterization Results by SEM, Rheology, and DSC Measurements for PP and PP/PS (70/30) Blends Uncompatibilized and Compatibilized with the PP-*g*-PS Graft Copolymers

Sample	d_n[a] (μm)	$\eta^*_{0.05\ rad/s}$[b] (10^4 Pa s)	$G'_{0.05\ rad/s}$[b] (Pa)	δ[b] (°)	T_c[c] (°C)	T_m[c] (°C)	$\Delta H_{m,whole}$[c] (J/g)	$\Delta H_{m,PP}$[d] (J/g)
PP	—	0.93	65	82.0	114.1	162.9	92.6	92.6
PP/PS	3.28	1.59	160	78.4	115.4	162.8	72.9	104.3
PP/PS/PP-7*g*-PS2.5-1	0.72	1.80	201	77.1	115.0	163.1	72.0	102.6
PP/PS/PP-7*g*-PS2.5-2.5	0.56	1.81	216	76.2	114.9	162.5	71.8	101.8
PP/PS/PP-7*g*-PS2.5-5	0.47	1.65	223	74.3	115.6	161.8	71.1	100.1
PP/PS/PP-7*g*-PS4.4-1	0.65	1.82	327	69.0	117.9	162.4	72.6	103.4
PP/PS/PP-7*g*-PS4.4-2.5	0.51	2.10	459	64.0	117.2	162.6	72.1	102.4
PP/PS/PP-7*g*-PS4.4-5	0.38	2.79	777	56.1	117.0	162.2	71.4	100.9
PP/PS/PP-7*g*-PS6.0-1	0.74	1.79	287	71.3	116.2	162.9	71.2	101.6
PP/PS/PP-7*g*-PS6.0-2.5	0.62	2.09	447	64.8	116.5	162.3	70.9	100.9
PP/PS/PP-7*g*-PS6.0-5	0.48	2.38	507	64.7	116.8	162.8	71.1	100.7

[a] Number-average diameter of PS particle, calculated from the SEM images.
[b] Determined by rheology measurements.
[c] Determined by DSC measurements.
[d] $\Delta H_{m,PP} = \Delta H_{m,whole}$/wt % of PP in the blend.

graft copolymers [see Figure 1(b,e,h) and Table II]. Furthermore, the PS particle size of PP/PS (70/30) blends compatibilized with 2.5 and 5 wt % PP-*g*-PS graft copolymer also decreased first and increased then with increasing the branch length of graft copolymer [see Figure 1(c,d,f,g,i,j) and Table II]. These results reveal that the branch length of PP-*g*-PS graft copolymer had opposite effects on its compatibilizing effect: on one hand, increasing the branch length could improve the compatibilizing effect of PP-*g*-PS graft copolymer on PP/PS blends, verified by the reduction of PS particle size; on the other hand, when the branch length exceeded a certain degree, further increasing the branch length of graft copolymer would weaken its compatibilizing effect. It is speculated that the melt viscosity of graft copolymer increased with increasing the branch length, which prevented it from migrating effectively to the interface of blend components.[1,32] However, some direct rheological evidence is still needed (discussed later).

Rheology of PP/PS Blends

The results of linear viscoelastic measurements can provide reliable information on the microstructure of the blends. The viscoelastic response of the blends at low shear frequencies can be used for evaluating the interfacial interaction between phases because the effect of flow-induced molecular orientation on viscosity and elasticity becomes less important.[33] However, to the best of our knowledge, the systematic investigation on rheological behavior of the PP/PS blends compatibilized with well-defined PP-*g*-PS graft copolymers has not been reported. Figure 3 shows the complex viscosity (η^*) versus angular frequency (ω) for the PP and PP/PS (70/30) blends uncompatibilized and compatibilized with PP-*g*-PS graft copolymers at 180°C, and the η^* values at 0.05 rad/s ($\eta^*_{0.05\ rad/s}$) are summarized in Table II. As shown in Figure 3 and Table II, the $\eta^*_{0.05\ rad/s}$ of uncompatibilized PP/PS (70/30) blend was higher than that of PP but lower than those of blends compatibilized with PP-*g*-PS graft copolymers. Compared to the compatibilized blends, the lower melt viscosity of uncompatibilized PP/PS (70/30) blend was probably due to the reason that the immiscibility between PP and PS prevented stress transfer across the interface and resulted in interfacial slippage.[33–35] When PP-*g*-PS graft copolymer was added to the blend, it improved the interfacial adhesion between PP and PS phases, which could account for the increase of $\eta^*_{0.05\ rad/s}$.

As can be seen from Figure 3(a) and Table II, the $\eta^*_{0.05\ rad/s}$ value of PP/PS/PP-7*g*-PS2.5-2.5 (70/30/2.5) blend was larger than those of both PP/PS/PP-7*g*-PS2.5-1 (70/30/1) and PP/PS/PP-7*g*-PS2.5-5 (70/30/5) blends. When the concentration of PP-7*g*-PS2.5 graft copolymer was above 2.5 wt %, a separate phase of PP-7*g*-PS2.5 graft copolymer may be formed, which would cause the reduction of η^*. Similar results were reported by Demarquette and coworker[3] and Kim and coworkers[36] for the PP/PS/SBS blend and the PP/SAN/PP-*g*-SAN blend (SAN: poly(styrene-*co*-acrylonitrile)), respectively. For the PP/PS/PP-7*g*-PS4.4 and PP/PS/PP-7*g*-PS6.0 blends, the $\eta^*_{0.05\ rad/s}$ increased with increasing the concentration of graft copolymers from 1 to 5 wt % [Figure 3(b,c)]. It is well established that only a small part of the compatibilizer is located at the interfacial area between the dispersed phase and the matrix, the rest distributing as micelles or micro-particles in either the matrix or the dispersed phase.[26] The $\eta^*_{0.05\ rad/s}$ values of PP-7*g*-PS4.4 and PP-7*g*-PS6.0 graft copolymers were much higher than those of the blend components (see Table I), so the part that distributed in PP matrix caused an increase in $\eta^*_{0.05\ rad/s}$. Therefore, the changing trend of rheological properties of PP/PS blends compatibilized with PP-*g*-PS graft copolymer depended on the compatibilizing effect as well as the rheological properties of the graft copolymer.

Figure 3(d–f) shows the η^* versus ω for PP/PS (70/30) blends compatibilized with the same concentration of three PP-*g*-PS

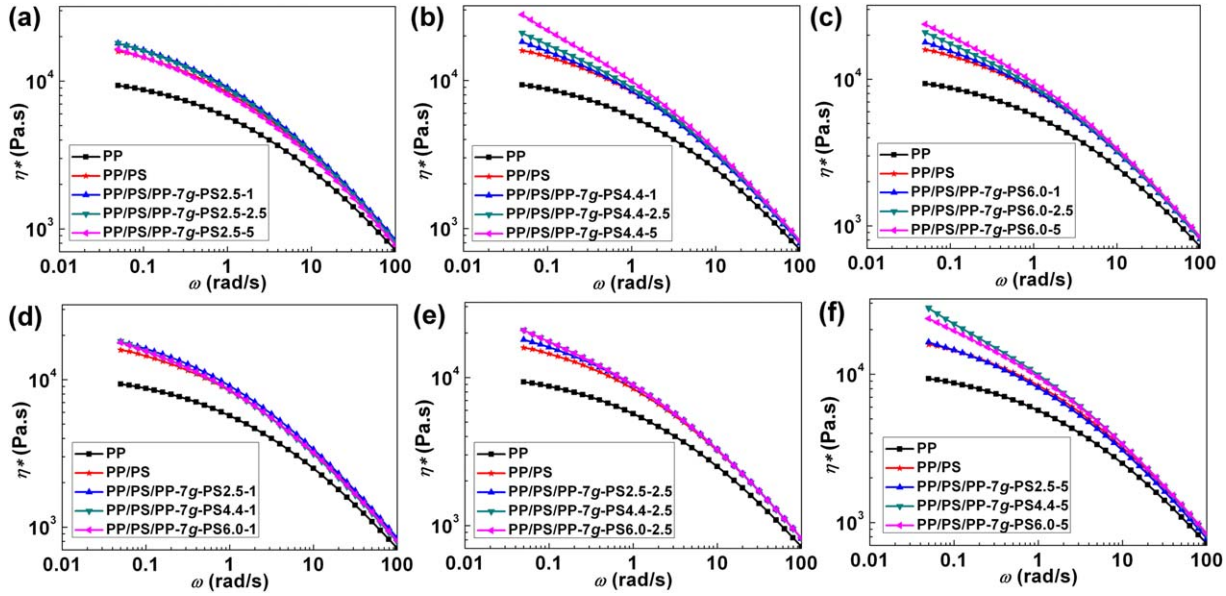

Figure 3. Complex viscosity versus angular frequency for the PP and PP/PS (70/30) blends uncompatibilized and compatibilized with the PP-*g*-PS graft copolymers at 180°C. [Color figure can be viewed in the online issue, which is available at wileyonlinelibrary.com.]

graft copolymers at 180°C. As shown in Figure 3(f) and Table II, the $\eta^*_{0.05\ rad/s}$ value of PP/PS/PP-7*g*-PS4.4-5 (70/30/5) blend was larger than that of PP/PS/PP-7*g*-PS2.5-5 (70/30/5) blend, implying that increasing the branch length of PP-*g*-PS graft copolymer could enhance the interfacial adhesion between PP and PS components. However, the $\eta^*_{0.05\ rad/s}$ value of PP/PS/PP-7*g*-PS6.0-5 (70/30/5) blend was smaller than that of PP/PS/PP-7*g*-PS4.4-5 (70/30/5) blend, which is a direct evidence for that the amount of graft copolymer located at the interfacial area decreased with the increase of branch length. Therefore, it is verified that the melt viscosity of PP-*g*-PS graft copolymer increased with increasing the branch length (see Table I), preventing the graft copolymer from migrating effectively to the interfacial region of PP/PS blends. This is the reason why the compatibilizing effect of PP-*g*-PS graft copolymer increased first and decreased then with increasing the branch length. Additionally, the $\eta^*_{0.05\ rad/s}$ of PP/PS (70/30) blend compatibilized with 1 and 2.5 wt % PP-*g*-PS graft copolymer exhibited a similar changing trend with increasing the branch length [Figure 3(d,e), and Table II]. These results confirm that the branch length of PP-*g*-PS graft copolymer had opposite effects on its compatibilizing effect.

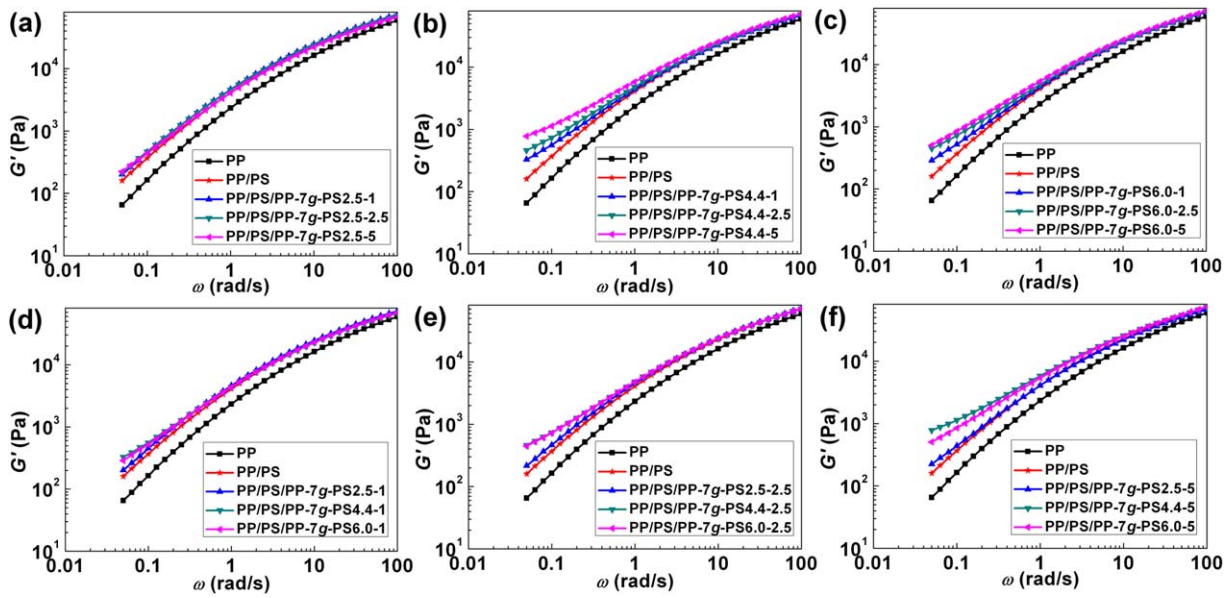

Figure 4. Storage modulus versus angular frequency for the PP and PP/PS (70/30) blends uncompatibilized and compatibilized with the PP-*g*-PS graft copolymers at 180°C. [Color figure can be viewed in the online issue, which is available at wileyonlinelibrary.com.]

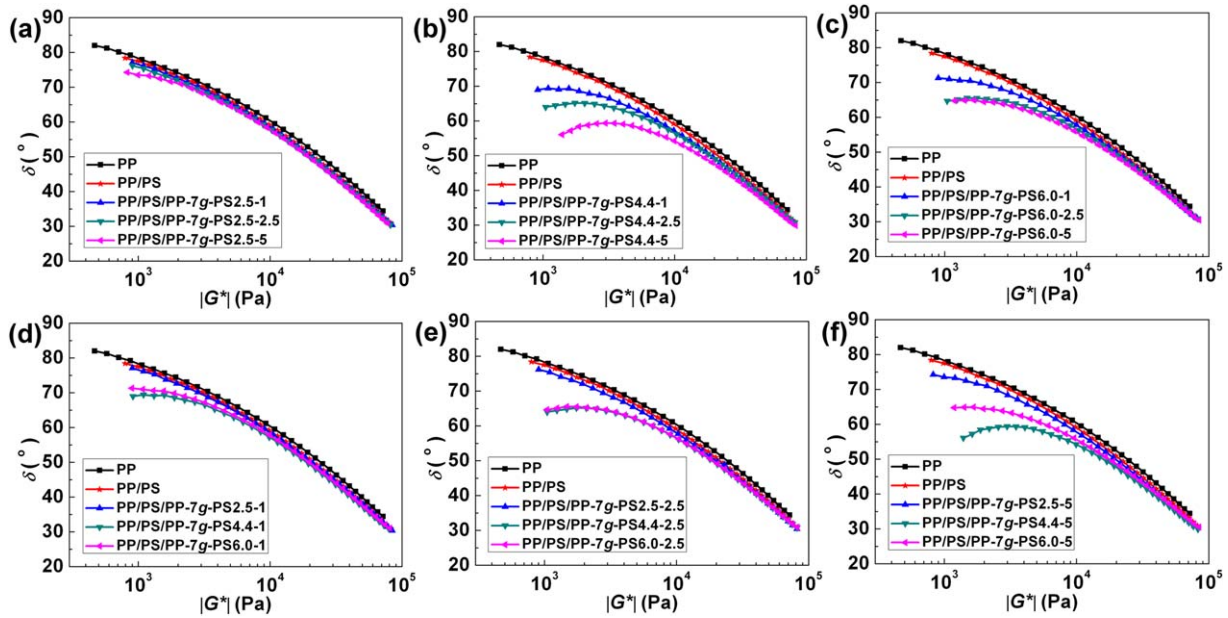

Figure 5. vGP plots of the PP and PP/PS (70/30) blends uncompatibilized and compatibilized with the PP-*g*-PS graft copolymers at 180°C. [Color figure can be viewed in the online issue, which is available at wileyonlinelibrary.com.]

Figure 4 shows the storage modulus (G') versus ω for PP and PP/PS (70/30) blends uncompatibilized and compatibilized with PP-*g*-PS graft copolymers at 180°C, and the G' values at 0.05 rad/s ($G'_{0.05\ \mathrm{rad/s}}$) are detailed in Table II. The $G'_{0.05\ \mathrm{rad/s}}$ of uncompatibilized PP/PS (70/30) blend was higher than that of PP but lower than those of the blends compatibilized with PP-*g*-PS graft copolymers. The PP-*g*-PS graft copolymer located at the interface and interacted with both the components, which restricted the chain mobility of the blend components and consequently increase the $G'_{0.05\ \mathrm{rad/s}}$ of the blends. Additionally, for all the compatibilized PP/PS (70/30) blends, $G'_{0.05\ \mathrm{rad/s}}$ value increased with increasing the concentration of PP-*g*-PS graft copolymers. As shown in Figure 4(d–f) and Table II, $G'_{0.05\ \mathrm{rad/s}}$ value of the PP/PS (70/30) blend compatibilized with the same concentration of PP-*g*-PS graft copolymer increased first and decreased then with increasing the branch length of graft copolymer. These results, in accordance with the changing trend of $\eta^*_{0.05\ \mathrm{rad/s}}$, further confirmed the aforementioned opposite effects of branch length on the compatibilizing effect of PP-*g*-PS graft copolymer.

The plot of loss angle δ ($\tan\delta = G''/G'$, G'' is the loss modulus) versus the absolute value of complex modulus ($|G^*|$) is the so-called vGP plot proposed by Van Gurp and Palmen.[37] It is known that materials are almost completely viscous when the δ terminal value is close to 90° and almost completely elastic when the δ terminal value is close to 0°. Figure 5 shows the vGP plots of PP and PP/PS (70/30) blends uncompatibilized and compatibilized with PP-*g*-PS graft copolymers at 180°C, and the δ terminal values are listed in Table II. As shown in Figure 5 and Table II, the δ terminal value of PP was close to 90°, indicating that PP melt was almost completely viscous. In addition, the δ terminal values of all PP/PS (70/30) blends were smaller than that of PP, and the δ terminal value of compatibilized PP/PS (70/30) blend decreased further with increasing the concentration of PP-*g*-PS graft copolymer. It indicates that the melt elasticity of uncompatibilized PP/PS (70/30) blend was higher than that of PP, and the melt elasticity of compatibilized PP/PS (70/30) blend increased further as the concentration of PP-*g*-PS graft copolymer increased. From Figure 5(d–f) and Table II, it can be observed that the melt elasticity of PP/PS (70/30) blends compatibilized with the same concentration of PP-*g*-PS graft copolymer increased first and decreased then with increasing the branch length of graft copolymer.

Thermal Properties of PP/PS Blends

Figure 6 shows the DSC curves of PP and PP/PS (70/30) blends uncompatibilized and compatibilized with PP-*g*-PS graft copolymers, and the results are summarized in Table II. As shown in Figure 6(a) and Table II, the crystallization temperatures (T_c) of uncompatibilized and compatibilized PP/PS (70/30) blends were higher than that of PP, suggesting that crystallization rate of PP increased after blending with PS. Moreover, the crystallization temperature of PP/PS (70/30) blends compatibilized with the same concentration of PP-*g*-PS graft copolymer slightly increased first and decreased then with the enhancement of branch length.

In addition, the melting temperatures (T_m) of PP and PP/PS (70/30) blends uncompatibilized and compatibilized with PP-*g*-PS graft copolymers were all around 163°C [Figure 6(b) and Table II]. The similarity of melting temperatures between PP and all the PP/PS (70/30) blends indicates that the PP lamellae thickness was almost identical. To estimate the net heat of fusion for the PP part, $\Delta H_{m,\mathrm{whole}}$ value can be normalized by the weight fraction of PP in the blend ($\Delta H_{m,\mathrm{PP}}$ in Table II). The obtained $\Delta H_{m,\mathrm{PP}}$ values of all the PP/PS (70/30) blends were a

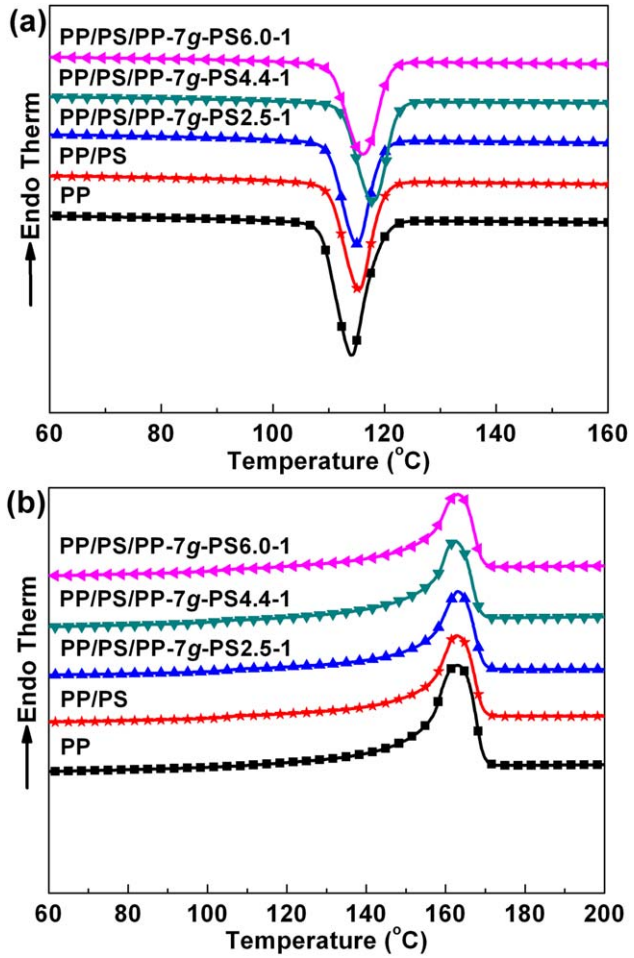

Figure 6. DSC cooling curves (a) and heating curves (b) of PP and PP/PS (70/30) blends uncompatibilized and compatibilized with PP-*g*-PS graft copolymers (DSC curves for the other samples were omitted for clarity). [Color figure can be viewed in the online issue, which is available at wileyonlinelibrary.com.]

little larger than that of PP, indicating that the presence of PS slightly increased the relative crystallinity of PP in the blends.

CONCLUSIONS

Three PP-*g*-PS graft copolymers with the same branch density but different branch lengths were employed to compatibilize PP/PS blends. The relationship between branch length and the compatibilizing effect of PP-*g*-PS graft copolymer on PP/PS blends were systematically investigated. The morphological and rheological studies of compatibilized PP/PS blends revealed that the PP-*g*-PS graft copolymers were effective in reducing the PS particle size and enhancing the interfacial adhesion between PP and PS phases. Furthermore, it is verified that the branch length of PP-*g*-PS graft copolymer had opposite effects on its compatibilizing effect: on one hand, increasing the branch length could improve the compatibilizing effect of PP-*g*-PS graft copolymer on PP/PS blends, demonstrated by the reduction of PS particle size and the enhancement of interfacial adhesion; on the other hand, increasing the branch length would increase the melt viscosity of PP-*g*-PS graft copolymer, which prevented it from migrating effectively to the interface of blend components. The crystallization temperatures (T_c) of uncompatibilized and compatibilized PP/PS (70/30) blends were higher than that of PP, suggesting that crystallization rate of PP increased after blending with PS. Additionally, the melting temperatures (T_m) of PP and PP/PS (70/30) blends uncompatibilized and compatibilized with PP-*g*-PS graft copolymers were almost the same, indicating that the PP lamellae thickness was almost identical. Furthermore, the presence of PS slightly increased the relative crystallinity of PP in the blends.

ACKNOWLEDGMENTS

Authors thank the financial support from the National Natural Science Foundation of China for the projects (no. 51233005 and 51073149).

REFERENCES

1. Li, J. G.; Li, H. Y.; Wu, C. H.; Ke, Y. C.; Wang, D. J.; Li, Q.; Zhang, L. Y.; Hu, Y. L. *Eur. Polym. J.* **2009**, *45*, 2619.
2. Caporaso, L.; Iudici, N.; Oliva, L. *Macromolecules* **2005**, *38*, 4894.
3. Macaubas, P. H. P.; Demarquette, N. R. *Polymer* **2001**, *42*, 2543.
4. Smit, I.; Radonjic, G. *Polym. Eng. Sci.* **2000**, *40*, 2144.
5. Li, Y.-Y.; Wang, Y.; Li, W.-Q.; Sheng, J. *J. Appl. Polym. Sci.* **2007**, *103*, 365.
6. Raghu, P.; Nere, C. K.; Jagtap, R. N. *J. Appl. Polym. Sci.* **2003**, *88*, 266.
7. Radonjic, G. *J. Appl. Polym. Sci.* **1999**, *72*, 291.
8. Halimatudahliana, A.; Ismail, H.; Nasir, M. *Polym. Test.* **2002**, *21*, 263.
9. Halimatudahliana, A.; Ismail, H.; Nasir, M. *Polym. Test.* **2002**, *21*, 163.
10. Li, Y.-Y.; Guo, C.; Zhao, Y.-H.; Chen, Z.-Q.; Sheng, J. *J. Macromol. Sci. Phys.* **2007**, *46*, 487.
11. Smit, I.; Radonjic, G.; Hlavata, D. *Eur. Polym. J.* **2004**, *40*, 1433.
12. Schulze, U.; Fonagy, T.; Komber, H.; Pompe, G.; Pionteck, J.; Ivan, B. *Macromolecules* **2003**, *36*, 4719.
13. D'Orazio, L.; Guarino, R.; Mancarella, C.; Martuscelli, E.; Cecchin, G. *J. Appl. Polym. Sci.* **1997**, *65*, 1539.
14. D'Orazio, L.; Guarino, R.; Mancarella, C.; Martuscelli, E.; Cecchin, G. *J. Appl. Polym. Sci.* **1999**, *72*, 1429.
15. Diaz, M. F.; Barbosa, S. E.; Capiati, N. J. *J. Polym. Sci. Part B: Polym. Phys.* **2004**, *42*, 452.
16. Diaz, M. F.; Barbosa, S. E.; Capiati, N. *J. Polymer* **2005**, *46*, 6096.
17. Li, R. B.; Zhang, X. Q.; Zhou, L. J.; Dong, J. Y.; Wang, D. J. *J. Appl. Polym. Sci.* **2009**, *111*, 826.
18. Adewole, A. A.; Denicola, A.; Gogos, C. G.; Mascia, L. *Adv. Polym. Technol.* **2000**, *19*, 180.

19. Adewole, A. A.; DeNicola, A.; Gogos, C. G.; Mascia, L. *Plast. Rubber. Compos.* **2000**, *29*, 70.
20. Park, E. S.; Jin, H. J.; Lee, I. M.; Kim, M. N.; Lee, H. S.; Yoon, J. S. *J. Appl. Polym. Sci.* **2002**, *83*, 1103.
21. Zhai, W. T.; Wang, H. Y.; Yu, J.; Dong, J. Y.; He, J. S. *J. Polym. Sci. Part B: Polym. Phys.* **2008**, *46*, 1641.
22. Fonagy, T.; Schulze, U.; Komber, H.; Voigt, D.; Pionteck, J.; Ivan, B. *Macromolecules* **2007**, *40*, 1401.
23. Lu, H. L.; Chung, T. C. *J. Polym. Sci. Part A: Polym. Chem.* **1999**, *37*, 4176.
24. Kaneko, H.; Matsuo, S.; Kawahara, N.; Saito, J.; Matsugi, T.; Kashiwa, N. *Macromol. Symp.* **2007**, *260*, 9.
25. Wang, L.; Yang, H. F.; Tan, H. Y.; Yao, K.; Gong, J.; Wan, D.; Qiu, J.; Tang, T. *Polymer* **2013**, *54*, 3641.
26. Chen, B.; Li, X. L.; Xu, S. Q.; Tang, T.; Zhou, B. L.; Huang, B. T. *Polymer* **2002**, *43*, 953.
27. Stary, Z.; Fortelny, I.; Krulis, Z.; Slouf, M. *J. Appl. Polym. Sci.* **2008**, *107*, 174.
28. Abad, M. J.; Ares, A.; Barral, L.; Cano, J.; Diez, F. J.; Garcia-Garabal, S.; Lopez, J.; Ramirez, C. *J. Appl. Polym. Sci.* **2004**, *94*, 1763.
29. Jeon, H. K.; Feist, B. J.; Koh, S. B.; Chang, K.; Macosko, C. W.; Dion, R. P. *Polymer* **2004**, *45*, 197.
30. Lu, B.; Chung, T. C. *Macromolecules* **1999**, *32*, 2525.
31. Wang, D.; Li, Y.; Xie, X.-M.; Guo, B.-H. *Polymer* **2011**, *52*, 191.
32. Xu, Y. W.; Thurber, C. M.; Lodge, T. P.; Hillmyer, M. A. *Macromolecules* **2012**, *45*, 9604.
33. Ares, A.; Silva, J.; Maia, J. M.; Barral, L.; Abad, M. *J. Rheol. Acta* **2009**, *48*, 993.
34. Zhao, R.; Macosko, C. W. *J. Rheol.* **2002**, *46*, 145.
35. Lu, Q. W.; Macosko, C. W. *Polymer* **2004**, *45*, 1981.
36. Sung, Y. T.; Han, M. S.; Hyun, J. C.; Kim, W. N.; Lee, H. S. *Polymer* **2003**, *44*, 1681.
37. Van Gurp, M.; Palmen, J. *Rheol. Bull.* **1998**, *67*, 5.